Proceedings of the 17th World Congress
The International Federation of Automatic Control
Seoul, Korea, July 6-11, 2008

Development of Integrated Alstom Gasification Simulator for Implementation Using DCS CS3000

A. Haryanto*, P. Siregar, D. Kurniadi**, and Keum-Shik Hong***

** School of Mechanical Engineering, Pusan National University;*
#30 Jangjeon-dong, Gumjeong-gu, Busan, 609-735, Korea;(e-mails: {a.haryanto, kshong}@pusan.ac.kr).
*** Department of Engineering Physics, Bandung Institute of Technology;*
#10 Ganesha, Bandung, 40132, Indonesia;(e-mails: {psiregar, kurniadi} @tf.itb.ac.id).

Abstract: In this paper we explore the development of integrated plant simulator that integrates MATLAB as an engine and DCS CS3000 as an industrial controller. It works realtime and online like real industrial control plant scheme. For industrial practicians like operator and engineer, this simulator is very useful as an operator training or control educational tools and can be used to implement loop pairing selection and tune the controller parameters. As a requirement of controlling using DCS, this paper provides integrated analysis tools for loop pairing by implementation relative gain array (RGA) method and decentralized relative gain (DRG). Plant case for this simulator is Alstom gasification.

Keywords : DCS CS3000, integrated simulator, Alstom gasification, pairing selection.

1. INTRODUCTION

In line with the complexity of industries, control problems also become more and more complex. It makes a challenge for university, especially in control area to solve and consider it and to integrate industrial aspects into teaching activity.

The main problem in providing practical control infrastructure for teaching activity is how expensive it is. It is related to providing control instruments and maintenance cost. Another needs in providing that infrastructure is the requirement of enough space that relatively difficult for several universities to provide it. For solving that problem, one way that can be taken is development of industrial simulator that represents real industry.

Recently, we can take advantages from rapid development of computer and communication protocol technology to develop plant simulator in computer. It is called as integrated plant simulator because this simulator integrates engine, data transfer communication via object-linked-embedded process control (OPC) technology and distributed control system (DCS) as a real industrial controller. Firstly, the simulator engine is developed in MATLAB, and then data is transferred via open system connectivity OLE for Process Control (OPC) technology and controlled by DCS CS3000.

For several decade, many developers have tried to build plant simulator using DCS, they are (Wanye et al., 2002; Geddes et al., 1998; and Nan Ye et al., 2000). They developed simulator inherently in DCS software, but in this research we develop simulator separately in MATLAB in order to obtain its proved numerical simulation so gives more accurate calculation and easiy to implement the control algorithm.

The contributions of this paper are: an integrated simulator consisting of a real controller, a real communication server, but a plant programmed in MATLAB is proposed. The second, integrated simulator also provides inputs-outputs pairing tools that enable control engineers to choose and simulate the best pairing of control loop based on RGA and sensitivity analysis of DRG. This pairing tool designed flexible and easy to be reconfigurable for any plant case. The resulted loop pairing, will be very useful for implementation of multi-loop controller in DCS.

2. SIMULATOR CONFIGURATION

The proposed integrated simulator is depicted in Fig. 1. It consists of three parts: an engine that provides the dynamics of the plant, a communication server that connects between the engine and control system, and a control system that performs distributed control. It is a hardware-in-the-loop simulation (HiLS) including the real controller and communication server, whereas the plant is modelled in software. In this paper, as an engine for solving the dynamics of the Alstom gasification plant, the MATLAB/Simulink is selected for its easiness of programming and graphical tools. As a communication server, an NI OPC is used. As a distributed control system, Yokogawa DCS CS3000, Japan, is used for monitoring and operation purposes.

2.1 Control System: DCS CS3000

The DCS CS 3000 of Yokogawa, Japan, is an integrated production control system, which is used to manage and control the operation of plants in a wide variety of industries including petroleum refineries, petrochemical, chemical,

pharmaceutical, food and beverages, paper and pulp, steel and non-ferrous metals, cement, power plant, gas, water and wastewater, and others (Yokogawa, 2007). The DCS mainly consists of three parts: field control station (FCS), human interface station (HIS), and V-Net data communication. The architecture of the DCS CS3000 adopted in this paper is depicted in Fig. 2. The system has a window based interface and a drag and drop function, and moreover provides an operation interface to other systems including production management systems, quality control systems, etc.

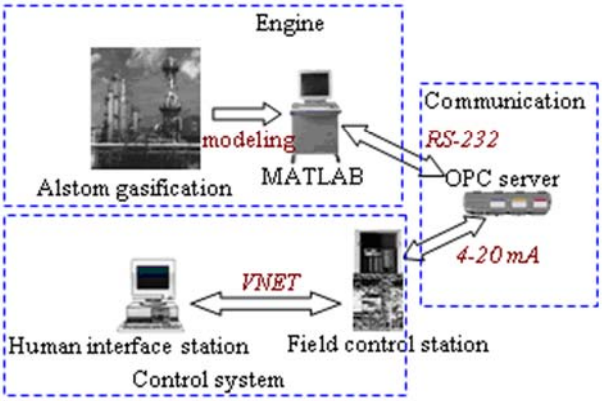

Fig. 1 Schematic of the proposed integrated simulation.

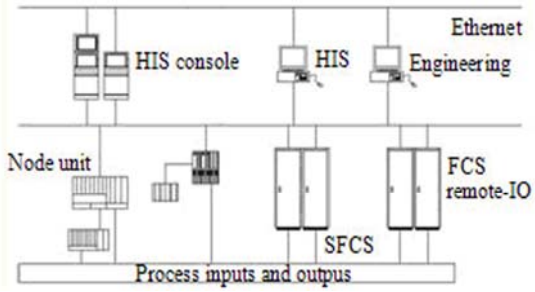

Fig. 2 The architecture of DCS CS3000

2.2. Communication: NI OPC Server

In order to access data from or to DCS CS3000, there are some issues to be considered, see Fig. 4. In the OPC framework, an application requesting data is referred to as an OPC client and an application providing data is referred to as an OPC server. Through the use of an NI OPC interface, it becomes possible to use an OPC server operating on an HIS to access various kinds of data on FCS stations and the HIS itself from OPC-compatible client applications operating on Windows machines. Moreover, it is possible to notify alarms which occurred in FCS and events. The type of OPC used in this paper is an OPC-data-access that has function to read and write plant data. Data produced by engine and written to DCS are y_1, y_2, y_3, and y_4 as process variables (PVs). Data read from DCS are u_1, u_2, u_3 and u_4 as manipulated variables (MVs). DCS conducts control algorithm based on PV data and setpoints (SVs) data. The explanation of data transfer scheme can be seen in Fig. 3.

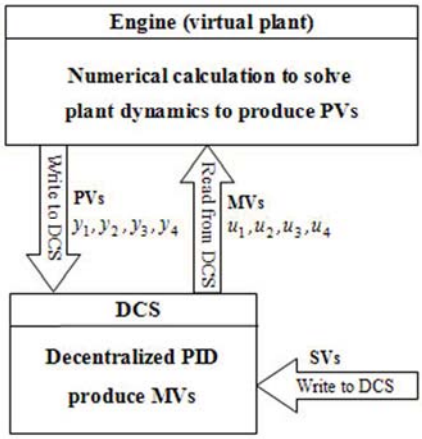

Fig. 3 Data transfer between Engine and DCS

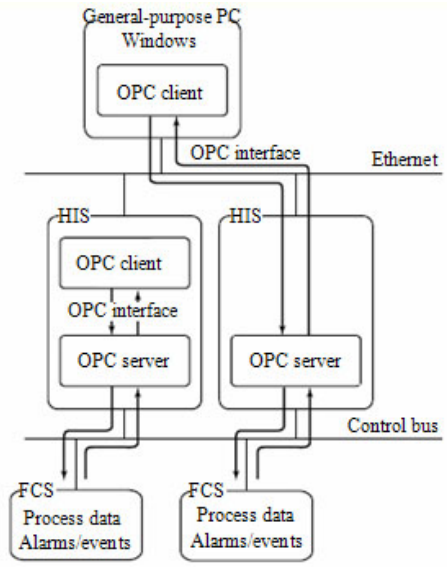

Fig. 4 The OPC frame-work on DCS CS3000

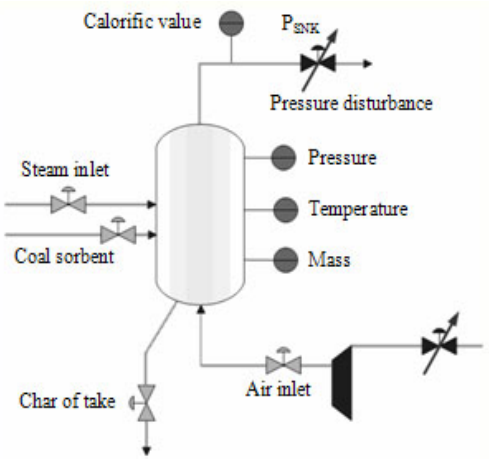

Fig. 5 Process flow diagram of the Alstom plant

2.3 Plant Model

In this paper, we use the Alstom gasification model, as our plant, that was obtained by (Moreea-Tahhaa, 2002; Rudy-

Zhang, 2006; and R. Dixon, 2006). Fig. 5 shows the process flow diagram of the Alstom plant. It is a multi-variable plant that consists of five control inputs (flow coal, irrigate flow mass, flow mass limestone, flow steam, and flow extraction char), four control outputs (gas value calorific, bed mass, fuel gas pressure, and fuel gas temperature), and one disturbance (sink pressure noted by P_{SNK} in Fig. 5).

The transfer function model of the Alstom plant are given by

$$\begin{bmatrix} y_1(s) \\ y_2(s) \\ y_3(s) \\ y_4(s) \end{bmatrix} = \begin{bmatrix} G_{11}(s) & G_{12}(s) & G_{13}(s) & G_{14}(s) \\ G_{21}(s) & G_{22}(s) & G_{23}(s) & G_{24}(s) \\ G_{31}(s) & G_{32}(s) & G_{33}(s) & G_{34}(s) \\ G_{41}(s) & G_{42}(s) & G_{43}(s) & G_{44}(s) \end{bmatrix} \begin{bmatrix} u_1(s) \\ u_2(s) \\ u_3(s) \\ u_4(s) \end{bmatrix} + \begin{bmatrix} G_{d1}(s) \\ G_{d2}(s) \\ G_{d3}(s) \\ G_{d4}(s) \end{bmatrix} P_{snk}$$

where P_{snk} is pressure disturbance (P_{SNK} in Fig. 5), $G_{ij}(s)$ and $G_{di}(s)$ can bee seen in appendix A.

Steady state and disturbance gain of the Alstom plant are given as follows

$$G(0) = \begin{bmatrix} 2.0565e5 & 3.1150e4 & -1.4821e5 & -1.12503e5 \\ -5.5598e3 & -6.6140e3 & 4.2170e3 & -830.3185 \\ -2.1626e4 & 1.6882e4 & -5.0155e3 & 5.1764e3 \\ 26.9683 & 30.3584 & -135.2488 & -47.6050 \end{bmatrix},$$

$$G_d(0) = \begin{bmatrix} -0.0124 & 0.0030 & 0.9234 & 2.381e-5 \end{bmatrix}^T.$$

These gains will be used in control structure selection and analysis.

3. CONTROL STRUCTURE SELECTION

In a DCS approach, the control structure has to be chosen in the way that the interaction among control loops is minimized. In the decentralized control approach, the loop configuration is the most important thing in order to achieve the best control performance of the plant. This means that the decision on what input is to be mainly used to control a certain output is more important than the selection of a control method or the design of control gains of the chosen control algorithm. If the control structure is improperly chosen, tuning of selected controllers will never reach a desired performance. In same case, mistakenly chosen control outputs and inputs will result in a limited performance, which this matter cannot be overcome by any tuning method and also any advanced controllers like MPC (Chen and McAvoy, 2003).

3.1 Loop Pairing Using the RGA Method

In this paper, we will try to implement the relative gain array (RGA) method, and then evaluate its performance by using the decentralized relative gain (DRG) compared to the currently implemented loop. The RGA equation formulated by Bristol (1966) is

$$\lambda_{ij} = \frac{\left[\frac{\partial CV_i}{\partial MV_j}\right]_{MV_k \text{Constant}}}{\left[\frac{\partial CV_i}{\partial MV_j}\right]_{CV_k \text{Constant}}} \quad (1)$$

where λ_{ij} is the RGA value, ∂CV_i is the change of the *i*-th controlled variable, ∂MV_j is the change of the *j*-th manipulated variable.

The loop pairing is selected in the way that the RGA value is close to one. Based on this approach, the loop pairing for the Alstom plant is proposed as follows:

$y_1 - u_3$ (Fuel Gas Calorific Value – Coal Flow),
$y_2 - u_1$ (Bed Mass – Char Extraction Flow),
$y_3 - u_2$ (Fuel Gas Pressure – Air Mass Flow),
$y_4 - u_4$ (Fuel Gas Temperature – Steam Mass Flow).

Which is different from the currently implemented loop pairing in the plant (Dixon, 2004) as

$y_1 - u_2$ (Fuel Calorific Value – Air Mass Flow),
$y_2 - u_3$ (Bed Mass – Coal Flow),
$y_3 - u_4$ (Fuel Gas Pressure – Steam Mass Flow),
$y_4 - u_1$ (Fuel Gas Temp. – Char Extraction Flow).

It is commented that the RGA approach is based on the assumption that the plant is controlled perfectly. This analysis is only based one steady state gain of the plant matrix.

3.2 Analysis of RGA Results Using DRG Properties

The RGA analysis has been proved for several plant cases, actually for 2x2 plant matrix (Bristol, 1966; Cui & Jacobsen, 2002). In this paper, we will compare the obtained loop pairing based on RGA and the currently implemented loop by using decentralized relative gain analysis (Schmidt & Jacobsen, 2003).

The DRG analysis relies on the problem of limited control bandwidth. In this approach, we do not need to define the controller type completely, but only by defining a measure of the achieved performance that is free from any particular controller, it is called independent design.

The critical frequency of the plant is the region around control bandwidth (ω_c) to achieve the desired performance. This ω_c then can be elaborated by some key specifications based on the frequency response like phase margin (Φ_m), gain cross over, and roll-off rate (n_{ro}). In control theory, this key specification then can be implemented by using the loop shaping theorem.

Using the internal model control (IMC) and the lead-lag compensator formulation, loop shaping theorem than defined by particular key specifier (f_i), which actually contains information about bandwidth frequency and cross over frequency of the plant. The formulation of $f_i(s)$ is

$$f_i(s) = \frac{1}{1 + l_i(s)} \tag{2}$$

where $f_i(s)$ is the performance specifier, $l_i(s)$ represents the desired open loop transfer function, which is defined as follows:

- When the roll-off rate n_{ro} = -1 (based on a lead-compensator scheme)

$$l_i(s) = \frac{k_i}{s}\frac{(s + bN)}{N(s + b)}, \tag{3}$$

where

$$b = \frac{\omega_c}{\sqrt{N}}, \tag{4}$$

$$k_i = \omega_c \sqrt{N}, \tag{5}$$

$$(\frac{\pi}{2} - \phi_m) = \tan^{-1}\left(\frac{\sqrt{N}}{2} - \frac{1}{2\sqrt{N}}\right). \tag{6}$$

- When n_{ro} roll-off rate = - 2 (based on IMC scheme)

$$l_i(s) = \frac{k_i \omega_c}{s}\frac{1}{1 + t_i(s)} \tag{7}$$

where

$$t_i = \frac{\tan(\frac{\pi}{2} - \phi_m)}{\omega_c}, \tag{8}$$

$$k_i = \left|1 + jt_i\omega_c\right|, \tag{9}$$

and t_i and k_i are time and gain integrator, respectively.

The DRG analysis has two interaction measures. They are the sensitivity interaction measure (X) and the disturbance sensitivity interaction measure (X_d), which are defined as follows:

$$X = \left[I + \overline{G}\,\widetilde{G}_m^{-1}((F^{-1} - I)^{-1} + \widetilde{A})^{-1}\right]^{-1}, \tag{10}$$

$$X_d = \left[I + \overline{G}\,\widetilde{G}_m^{-1}((F^{-1} - I)^{-1} + \widetilde{A})^{-1}\right]^{-1} G_d \tag{11}$$

where $\overline{G}$ is an off-diagonal matrix, $\widetilde{G}_m$ is resulted from the separation of the system $\widetilde{G}$ into a diagonal all pass transfer matrix $\widetilde{A}$ and a diagonal minimum phase system $\widetilde{G}_m(s)$. So that $\widetilde{G} = \widetilde{A}\widetilde{G}_m$

where

$\widetilde{G}$ is diag (G), and

G_d is disturbance gain.

The RGA result when evaluated by DRG approach shows that the loop pairing from (Dixon, 2000) is better than the RGA pairing. At certain bandwidth frequency, the RGA pairing is more sensitive to other loops and also more sensitive to the presence of disturbances (see Fig. 5 and Fig. 6).

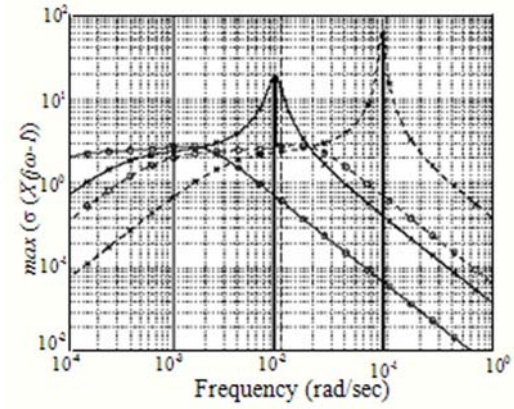

Fig. 6 Sensitivity Interaction Measure
-xxx- y_1 - u_3 (RGA); -ooo- y_1 - u_2

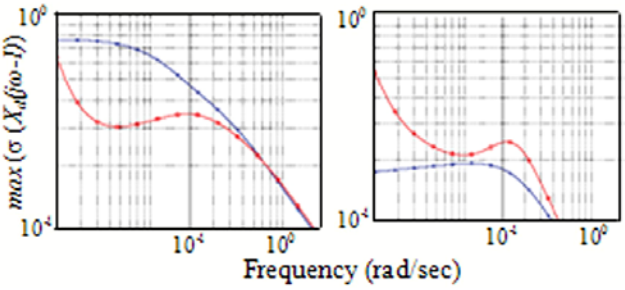

Fig. 7 Disturbance Sensitivity Interaction Measure
Left : -xxx- y_1 - u_3 (RGA); -ooo- y_1 - u_2 (R. Dixon)
Right : -xxx- y_3 - u_2 (RGA); -ooo- y_3 - u_4 (R. Dixon)

4. SIMULATION RESULTS

Control performance is evaluated by set point tracking and disturbance rejection test for RGA pairings and the currently implemented pairing when controlled using DCS. Control of the Alstom gasification plant using DCS indicates that the currently implemented loop control gives better in performance responses (tracking the setpoint and attenuating the disturbance) then RGA which the maximum absolute error (MAE) 5069 for y_1, 8.455 for y_2 is, 5782 for y_3 and 0.2664 for y_4. RGA pairing is 5855 for y_1, 8.455 for y_2, 7714 for y_3 and 0.3232 for y_4. Some simulation results can be found in Appendix B Fig. 8 – 11, the noises appearing are from real data transfer communication using 4-20 mA and ADDA conversion.

5. CONCLUSIONS

Integrated plant simulator is very helpful in conducting plant operation training for engineer and operator such as modifying control loop configuration and tuning the controller parameters. Studies in this paper also indicate that using RGA analysis is not effective in control structure selection for Alstom gasification plant.

ACKNOWLEDGMENT

This work was supported by the Regional Research Universit ies Program (Research Center for Logistics Information Tech nology, LIT) granted by the Ministry of Education & Human Resources Development, Korea.

REFERENCES

Bristol, E.H. (1966). *On a new measure of interactions for multivariable process control*. IEEE Transactions on Automation Control, vol. 11, no. 1, pp. 133-134.

Chen R. and McAvoy, T.J. (2003). *Plantwide Control system design: Methodology and application to a vinyl acetate process*. Ind . Eng. Chem. Res. vol. 42, pp. 4753 - 4771.

Cui H., and Jacobsen E.W., (2002). *Performance limitations in decentralized control*. Journal of Process Control, vol. 12 (4), page 485–494.

Dixon, R., Pike, A. and Donne, M. (2000). *The ALSTOM benchmark challenge on gasifier control*. Proc. Inst. Mech. Eng. I, J. Syst. Control Eng.. 214, pp. 389–394.

Geddes, D.J, Bailie, A.P.H., Cregan, M., and Swidernbank, E. (1998), *A Realtime Simulation of A 200 MW Thermal Power Plant for Optimising Combustion Engine*. UKACC International Conference on Control.

Henning Schmidt and Elling W. Jacobsen, 2003. *Selecting control configurations for performance with independent design*. Journal of Computers and Chemical Engineering, 27, pp. 101-109.

Moreea- R.Tahha, (2002). *Modeling and simulation for coal gasifier in fluidised bed*, Journal of Fuel, no. 81, pp. 1687-1702.

Nan Ye, Sairam Valluri, Mitch Barker, Po-Yang Yu, (2000). *Integration of advanced process control and full scale dynamic simulation*. ISA Transactions, 39, pp. 273-280, 2000.

Rudy, A. and Jie Zang, (2006). *Control Structure Selection for The Alstom Gasifier Benchmark Process Using GRGD Analysis*. Paper in American Control Conference (ACC).

Technical Information, (2007). *CENTUM CS 3000 integrated production control system overview*. Yokogawa Electric Corp., Japan.

Wanye Y., Han Pu, Yang Mingyu and Zhaou Lihui, (2002). *The implementation of power plant simulator based on distributed control system*, Proc. IEEE Tencon.

Appendix A. Transfer function matrix of Alstom plant

$$\begin{bmatrix} y_1(s) \\ y_2(s) \\ y_3(s) \\ y_4(s) \end{bmatrix} = \begin{bmatrix} G_{11}(s) & G_{12}(s) & G_{13}(s) & G_{14}(s) \\ G_{21}(s) & G_{22}(s) & G_{23}(s) & G_{24}(s) \\ G_{31}(s) & G_{32}(s) & G_{33}(s) & G_{34}(s) \\ G_{41}(s) & G_{42}(s) & G_{43}(s) & G_{44}(s) \end{bmatrix} \begin{bmatrix} u_1(s) \\ u_2(s) \\ u_3(s) \\ u_4(s) \end{bmatrix} + \begin{bmatrix} G_{d1}(s) \\ G_{d2}(s) \\ G_{d3}(s) \\ G_{d4}(s) \end{bmatrix} P_{snk}(s)$$

where

$$G_{11}(s) = \frac{288.5s + 0.1317}{s^2 + 0.0009365\ s + 6.404e-7},$$

$$G_{21}(s) = \frac{-1.083s + 0.001157}{s^2 + 0.0007612\ s + 2.081e-7},$$

$$G_{31}(s) = \frac{10.88s - 0.001422}{s^2 + 0.0006466\ s + 6.668e-8},$$

$$G_{41}(s) = \frac{0.06393\ s + 9.769e-6}{s^2 + 0.0007962\ s + 3.623e-7},$$

$$G_{12}(s) = \frac{-6927\ s + 1.95}{s^2 + 0.04927\ s + 6.26e-5},$$

$$G_{22}(s) = \frac{-0.428s + 0.000201}{s^2 - 0.0003426\ s - 3.039e-8},$$

$$G_{32}(s) = \frac{2444\ s + 6.16}{s^2 + 0.2465\ s + 0.0003653},$$

$$G_{42}(s) = \frac{0.04664\ s + 1.779e-5}{s^2 + 0.001197\ s + 5.86e-7},$$

$$G_{13}(s) = \frac{5303\ s - 6.382}{s^2 + 0.03362\ s + 4.306e-5},$$

$$G_{23}(s) = \frac{0.5327\ s + 0.001158}{s^2 + 0.001245\ s + 2.746e-7},$$

$$G_{33}(s) = \frac{1039\ s - 1.618}{s^2 + 0.2468\ s + 0.0003226},$$

$$G_{43}(s) = \frac{-0.05418\ s + 1.318e-5}{s^2 + 0.0005866\ s - 9.745e-8},$$

$$G_{14}(s) = \frac{5035\ s - 1.029}{s^2 + 0.02635\ s + 8.23e-6},$$

$$G_{24}(s) = \frac{-0.7753\ s - 0.004223}{s^2 + 0.007574\ s + 5.086e-6},$$

$$G_{34}(s) = \frac{4800\ s + 0.4871}{s^2 + 0.3032\ s + 9.41e-5},$$

$$G_{44}(s) = \frac{-0.005225\ s - 4.671e-5}{s^2 + 0.00226\ s + 9.812e-7},$$

$$G_{d1}(s) = \frac{0.02226\ s - 2.345e-6}{s^2 + 0.06238\ s + 0.0001897},$$

$$G_{d2}(s) = \frac{1.764e-6s - 1.04e-9}{s^2 + 6.625e-5s - 3.419e-7},$$

$$G_{d3}(s) = \frac{0.3813\ s + 0.001229}{s^2 + 0.411s + 0.001331},$$

$$G_{d4}(s) = \frac{-1.237e-7s + 9.687e-12}{s^2 + 0.001347\ s + 4.068e-7}.$$

Apendix B Simulation Results

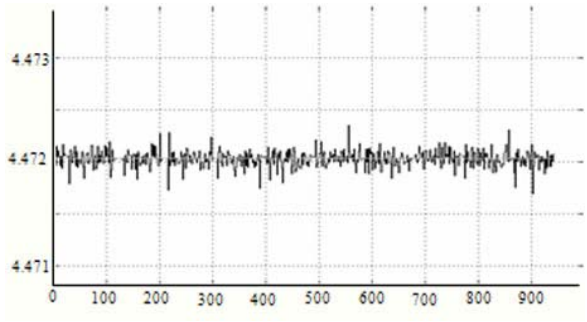

(a). Dixon pairing

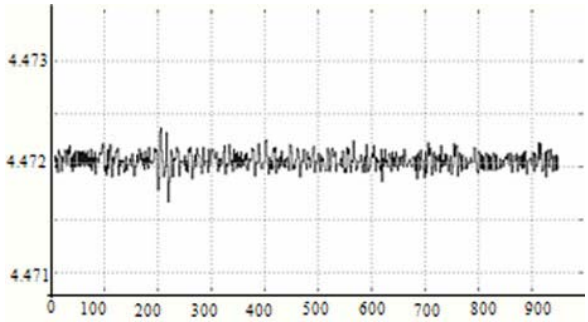

(b). RGA pairing

Fig. 8 Fuel calorific value response

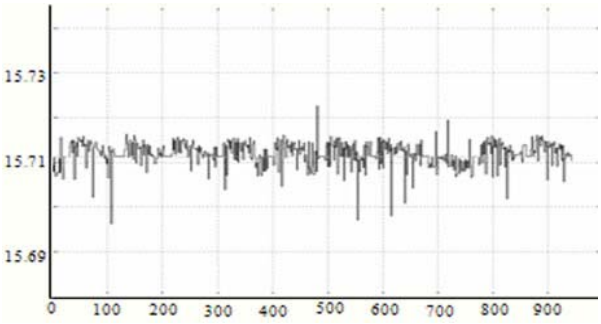

(a). Dixon pairing

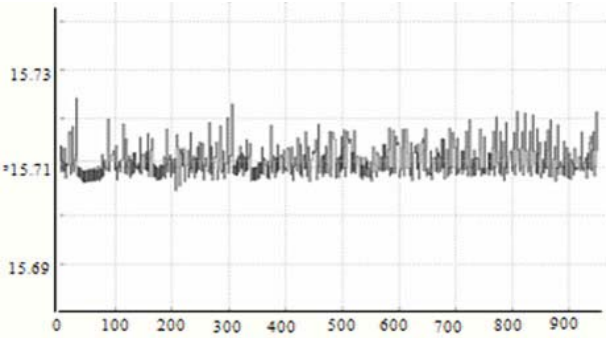

(b. RGA pairing

Fig. 9 Pressure response

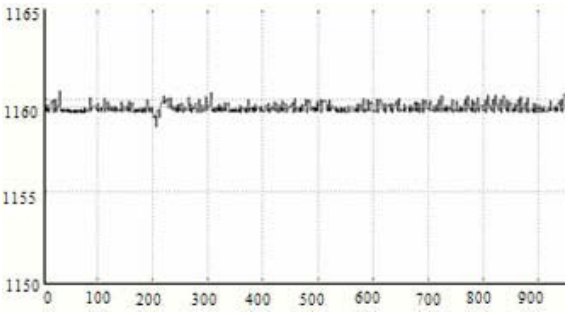

(a) Dixon pairing

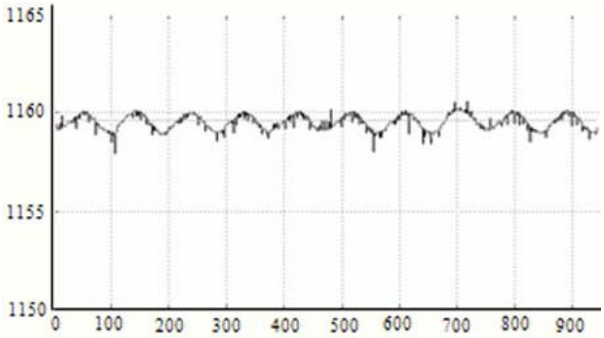

(b) RGA pairing

Fig. 10 Temperature response

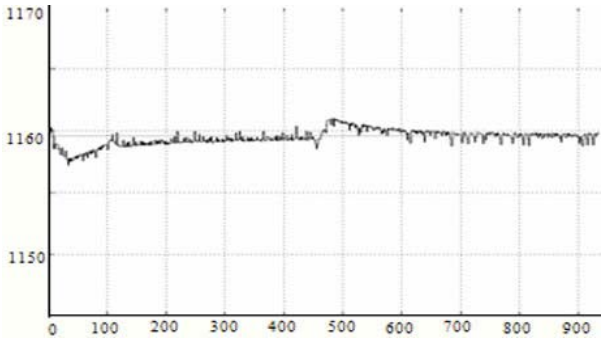

(a) Dixon pairing

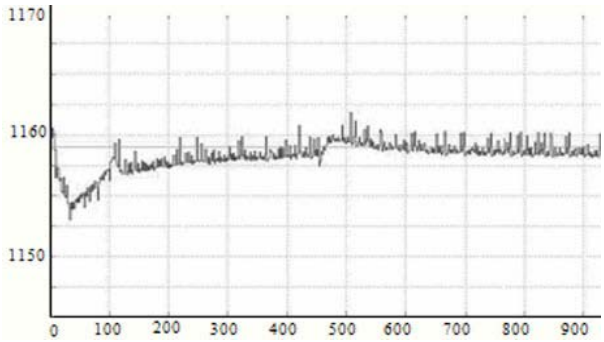

(b) RGA pairing

Fig. 11 Temperature response to step pressure disturbance